# Analysis of spacing of streaky structures within surface layer above real urban

Ayako Yagi[1], Atsushi Inagaki[2], Manabu Kanda[3], Chusei Fujiwara[4], and Yasushi Fujiyoshi[5]

[1]*Tokyo Institute of Technology, Department of International Development Engineering, Tokyo, Japan*
[2]*Tokyo Institute of Technology, Department of International Development Engineering, Tokyo, Japan*
[3]*Tokyo Institute of Technology, Department of International Development Engineering, Tokyo, Japan*
[4] *Meteorological Research Institute, Tsukuba, Japan*
[5] *Institute of Low Temperature Science, Hokkaido University, Sapporo, Japan*

dated : 15 June 2015

## 1. Introduction

Coherent structures of turbulence within the atmospheric surface layer highly contributes momentum, heat and scalar transportation near the ground. However, its spatial characteristics in urban area are still not well investigated. This paper focused on the streaky pattern of coherent structures (horizontal roll vortices and streaks) within the urban surface layer, which is observed by a three-dimensional scanning coherent Doppler lidar (3D-CDL).

Horizontal roll vortices and streaks are different nature, although both of two show similar streaky patterns almost along the stream-wise direction visible in the horizontal velocity distribution. Horizontal roll vortices have been mainly investigated in the field of meteorology (Deardorff 1972; Sykes and Henn 1989). Mostly, horizontal roll vortices are observed within the mixed layer due to the deformation of the Benard cell convection by vertical shear. Meanwhile, streaks have been studied in the field of the fluid mechanics. Streaks within the neutral boundary layer are considered to be composed of packets of hairpin vortices (Adrian et al. 2001). Few papers have investigated both of roll vortices and streaks comprehensively. Moeng and Sullivan (1994), Khanna and Brasseur (1997) and Castillo et al. (2011) pointed out the coexistence of horizontal roll vortices and streaks using LES.

The objective of this study is to investigate streaky patterns in the atmospheric turbulence which include horizontal roll vortices and streaks above an urban area qualitatively and quantitatively in terms of (1) examination of the atmospheric condition when streaky pattern appears and (2) the quantification of the spacing of streaks. A 3-months observation using the 3D-CDL and a sonic anemometer was conducted in the urbanized area, Tokyo Japan. Thanks to the long-term observation, various kinds of flow patterns were observed, including turbulent coherent structures (the Benard cell convection, horizontal roll vortices and streaks) and non-coherent structures. Through the classification of all possible flow patterns, the atmospheric conditions when the streaky patters appear are specified.

## 2. Observation

A field observation using 3D-CDL and a sonic anemometer was carried out in Tokyo, Japan. The specifications of the 3D-CDL are shown in Table 1. The 3D-CDL scans the atmosphere with an eye safe laser whose wavelength is 1.54 μm. The maximum range is 4275 m and the range resolution is 50 m. Our scanning sequence consists of both of horizontal scannig (PPI; Plan Position Indicator) and vertical scanning (RHI; Range Height Indicator) (Table 2). The tangential resolutions of PPI and RHI are about 1.2 degree and 1.3 degree respectively, which is decided by a pulse repetition frequency, pulse hits and a scan speed.

The 3D-CDL was installed on the roof top of the building at the height of 55 m above ground level (Figure 1). The dominant land use which is covered by our 3D-CDL is densely-built up area including several high buildings and low residential buildings (Figure 1). A sonic anemometer was also installed on the roof top of the building which is 500 m far from the 3D-CDL at the height of 25 m from the ground (Figure 1). Three components of wind velocity and temperature were sampled at 10 Hz.

## 3. Methodologies

### 3.1 Visual classification of flow patterns

Snapshots of the radial velocity distribution measured by the 3D-CDL show various kinds of flow patterns. Then,we visually classified them into six groups; *Streak, Mixed, Fishnet, No streak, Front, The others*. The criteria and representative radial velocity distribution in each flow pattern shown in Table 3 and Figure 2. The criteria of the classification is the shape of the boundary between positive and negative radial velocity and the pattern in the

radial velocity. *Streak*, *Mixed* and *Fishnet* represents velocity fluctuation by turbulent structures. *The streak* is streaky coherent structures almost along stream-wise, which correspond to horizontal roll vortices or streaks. *Fishnet* is convective cell circulation (Fujiwara et al. 2011). In contrast, *No streak* doesn't have clear patterns in radial velocity, which corresponds to the flow with few coherent structures. *The others* contains various kinds of pattern (e.g. Figure 2(f) shows the wavy pattern in the boundary between positive and negative radial velocity).

We visually classified snapshots of the horizontal velocity distribution measured by PPI scanning during two seasons; autumn (from 25th Sep 2012 to 31th Oct 2012) and winter (from 1st Nov 2012 to 31th Dec 2012). Snapshots with containing a lot of error which had a smaller signal to noise ratio were removed as *Error* for the data quality management. In addition, the snapshot with rain were treated as *Rain*.

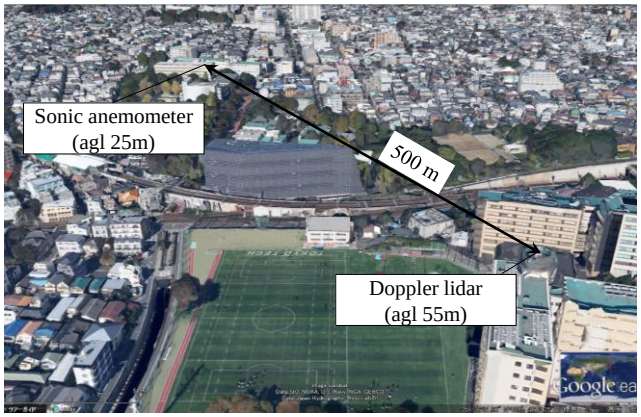


*Fig. 1 Deployment of instruments*.

*Table. 1 Specifications of the 3D-CDL.*

| | |
|---|---|
| Wavelength | 1.54 μm |
| Laser pulse energy | 0.5 mJ/pulse |
| Laser pulse width | 213±10 ns |
| Pulse repetition | 4 kHz |
| Range resolution | 50 m |
| Minimum range | 325 m |
| Maximum range | 4275 m |

*Table. 2 Criteria of visual classification.*

| | |
|---|---|
| *Streak* | Clear streaky patterns almost along dominant wind direction.<br>The boundary of positive and negative radial velocity is straight. |
| *Mixed* | Streaky patterns almost along dominant wind direction.<br>The boundary of positive and negative radial velocity is distorted. |
| *Fishnet* | Periodic cell-like (fishnet) pattern.<br>The lines of 0 m $s^{-1}$ radial velocity are patchy. |
| *No streak* | Non-streaky pattern along dominant wind direction.<br>The boundary of positive and negative radial velocity is straight. |
| *Front* | Clear convergence line. |
| *The others* | Exception to the above four groups. |

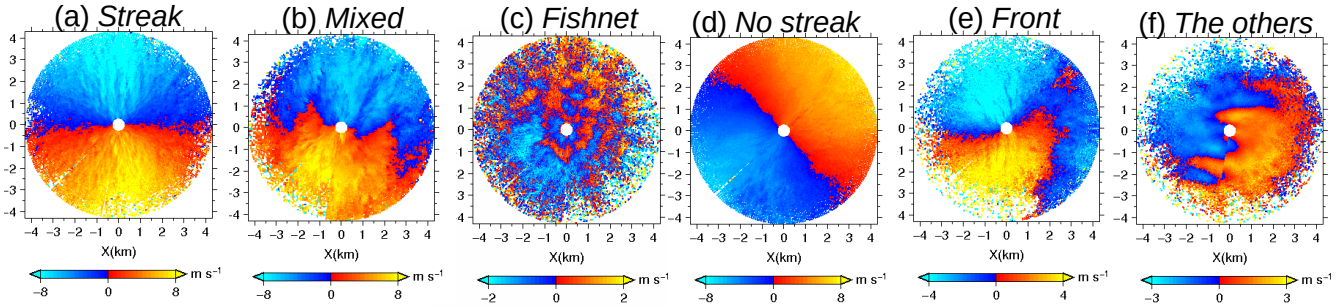


*Fig. 2 Snapshot of representative flow patterns measured by PPI scanning of the 3D-CDL.*

### 3.2 Turbulent statistics

The turbulent statistics below are calculated by applying the eddy correlation method for the wind velocity and temperature measured by the sonic anemometer;

$$u_* = (-\overline{u'w'})^{1/2}, \quad (1)$$

$$T_* = -\overline{w'T'}/u_*, \quad (2)$$

$$\frac{z}{L} = \frac{u_*^2 z}{\kappa(g/T)T_*}. \quad (3)$$

where $u$ is streamwise velocity, $w$ is vertical velocity, $T$ is temperature, $u_*$ is friction velocity, $T_*$ is friction temperature, $L$ is Monin-Obukhov length, $z$ is the height from the ground, $\kappa$ is Karman constant, $g$ is gravitational acceleration. Bar and prime mean temporal average for 30-minutes and fluctuation component from averaged value respectively.

### 3.3 Estimtation of the spacing of streaky structures

The spacing of streaky structures (λ) was estimated quantitatively for the cases which was classified into *Streak* in our visual classification. Figure 3 (a) (b) shows two cases of raw radial velocity distribution; which are thicker and thinner streaky patterns. Table 3 shows the atmospheric conditions when the flow patterns in Figure 3 were observed. λ is examined in the black rectangle areas shown in Figure 3 (a) (b), which are 3200m by 1000m, respectively. Firstly, radial velocity fluctuation in the area were calculated by subtracting spatial mean radial velocity from raw radial velocity (Figure 3 (c) (d)). Next, λ was decided from the peak wavelength of a power density spectrum which was calculated from the fluctuation of radial velocity along each spanwise. The values of λ used in Figure 6 are averaged for 30 minutes including 9 snapshots.

## 4. Results

### 4.1 Occurrence condition of flow patterns

Table 4 shows the occurrence number of flow patterns in autumn and winter which were visually classified. The occurrence percentage of *Streak* is the highest in both of two seasons. Percentages of it in autumn and winter are 59% and 52% respectively. Percentages in the other flow patterns are different in two seasons. The second frequent flow pattern in autumn is *Mixed* and one in winter is *No streak*. Besides, the share of *No streak* and *The others* in winter are larger than one of autumn. *Fishne*t which is convective cell circulation driven by buoyancy were observed not only autumn but also winter.

Figure 4 shows the diurnal variation of the occurrence number of each flow patterns and averaged heat flux ($\overline{w'T'}$) in two seasons. *Streak* appears throughout the whole day. In contrast, *Mixed* and *Fishnet* mainly appear during daytime when $\overline{w'T'}$ is positive and *No streak* and *The others* mainly appears during nighttime when $\overline{w'T'}$ is negative. This result suggests that the heat flux (buoyancy) is one of the important factors to explain the occurrence condition of each flow pattern.

Figure 5 shows the relationship between atmospheric stability and horizontal wind speed ($U$) for each flow pattern. Here, $U$ is spatially averaged horizontal wind speed at 55 m which is estimated by velocity azimuth method. Each plot is an averaged value for 30-minutes. In the neutral and unstable cases, *Fishnet* appears in more unstable stratification with smaller horizontal wind speed, whereas *Steak doe*s in near neutral with larger horizontal wind speed. *Mixed* are plotted between *Fishnet* and *Streak.* Under stable stratification, *Steak appears* in near neutral with larger horizontal wind speed, as was expected.With increasing stable stability ($-z/L > 0.1$), however, the share of *Streak* decreases and non-coherent structure like *No streak* and *The others* become dominant.

### 4.2 Characteristics of spacing of streaky patterns

Figure 6 shows the relationship between spacing of streaky structure (λ) and three meteorological variables such as horizontal wind speed ($U$) , wind shear ($\Delta U/\Delta z$) and atmospheric stability ($z/L$). The plots are separated as;(a)(b)(c)(d) include all 1325 cases, (e)(f)(g)(h) include 524 cases when $U$ is larger than $6\ \mathrm{m\ s^{-1}}$ and (i)(j)(k)(l) include 392 cases when $U$ is larger than $6\ \mathrm{m\ s^{-1}}$.The last group do not include the cases around sunset time (16:00-20:00 in local time). Here, the definition of $U$ is the same as in section 4.1. The variable $\Delta U/\Delta z$ is the difference of horizontal mean wind speed between 75 m and 175 m above the ground level, which is estimated by composing the radial velocity distribution on two orthogonal slices perpendicular to the ground.

The variable λ becomes smaller with increasing $\Delta U/\Delta z$ (Figure 6 (f)). A plot during a typhoon (open circle), which is the case of extremely large horizontal wind speed, also follows this relationship, meanwhile it is far from the other plots if it is plotted on $U$ (Figure 6 (e)). This means that λ is affected by the magnitude of wind shear, not one of wind speed. Additionally, large eddy simulation of a realistic urban geometry (Nurul 2015) also reproduced a similar value as our field observation (Figur 6 (f)).

By eliminating the cases around sunset, we can see a clearer correlation between λ and $z/L$ (Figure (k)(l)) than in the cases including sunset (Figure (g)(h)). This implies that the coherent structures which developed before sunset still remain and keep the size at the measurement height, although the stability near the ground changed into neutral or stable. The relationship between λ and $z/L$ in this observation is comparable to the results from dual-Doppler ldiar observation conducted by Newsom et al (2008). They also observed that λ gets smaller when the atmospheric stability becomes more stable.

## 5. Conclusions

The flow patterns and the spacing of streaky structure over real urban were investigated based on by 3-month observation by the 3CDL and a sonic anemometer. The snapshots of horizontal velocity distribution were visually classified, and their characteristics were examined. In addition, the spacing of streaky structures was estimated and evaluated their dependence on atmospheric conditions. The followings are the substantial outcome of this study;

1) The occurrence percentage of *Streak* dominates more than 50 % in both autumn and winter.
2) *Streak* occurs in the various atmospheric condition with the exception with strongly unstable or stable stratification.
3) The spacing of streaky structures becomes smaller with increasing wind shear in the case when $U$ is greater than $6\ \mathrm{m\ s^{-1}}$.
4) The spacing of streaky structures becomes smaller as the atmospheric condition becomes more stable in the case that $U$ is greater than $6\ \mathrm{m\ s^{-1}}$ excluding the cases around sunset time.

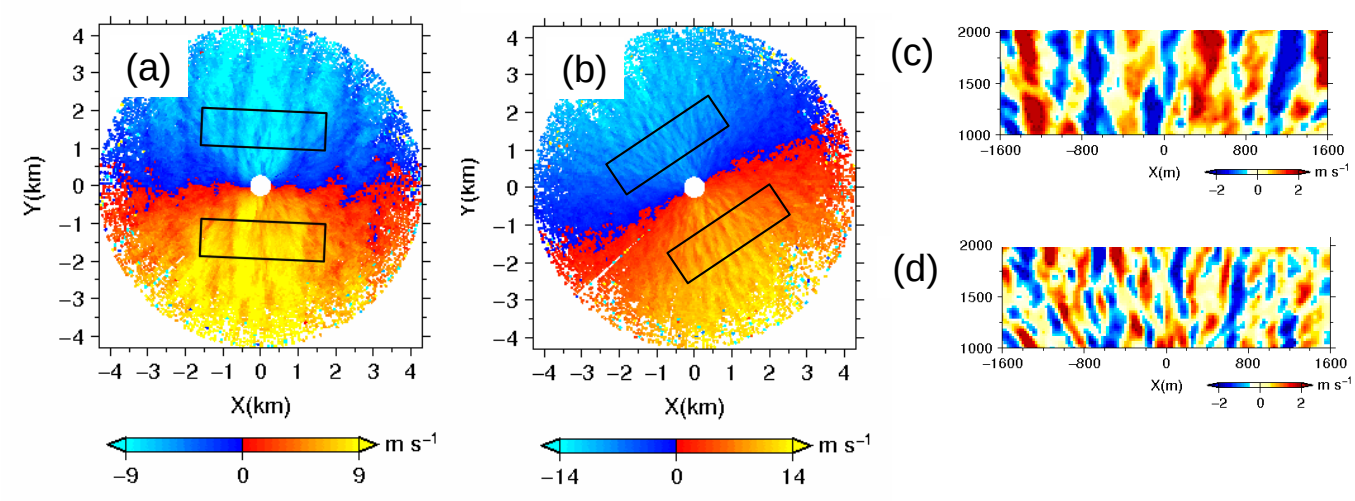


*Fig. 3 Sample of streaky patterns. (a)(b)raw radial velocity, (c)(d)fluctuation of radial velocity.*

*Table. 3 Atmospheric parameters of streaky patterns shown in Figure3.*

| | $U$ (m s$^{-1}$) | $u_*$ (m s$^{-1}$) | $T_*$ (K s$^{-1}$) | $z/L$ | $\Delta U/\Delta z$ (s$^{-1}$) | $\lambda$ (m) |
|---|---|---|---|---|---|---|
| (a) 27th Sep 9:45 | 8.4 | 0.68 | -0.027 | -0.047 | 0.009 | 567 |
| (b) 10th Nov 2:45 | 10.6 | 0.64 | 0.065 | 0.022 | 0.041 | 326 |

*Table. 4 Occurrence numbers of flow ptterns.*

| | *Streak* | *No streak* | *Mixed* | *Fishnet* | *Front* | *The others* | total of analysis target | *Error* | *Rain* | total of non-analysis target |
|---|---|---|---|---|---|---|---|---|---|---|
| autumn 9/25~10/31 | 5,612 (59%) | 1,413 (15%) | 1,620 (17%) | 291 (3%) | 52 (0.5%) | 513 (5%) | 9,459 | 1,338 (81%) | 317 (19%) | 1,655 |
| winter 11/1~12/31 | 4,751 (52%) | 2,021 (22%) | 1,159 (13%) | 319 (4%) | 13 (0.1%) | 887 (10%) | 9,150 | 7,335 (94%) | 501 (6%) | 7,836 |
| Total | 10,363 (56%) | 3,434 (18%) | 2,779 (15%) | 610 (3%) | 65 (0.3%) | 1,400 (8%) | 18,651 | 8,673 (91%) | 818 (9%) | 9,491 |

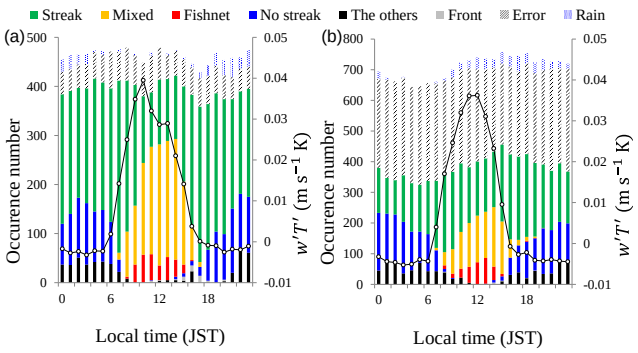


*Fig. 4 Diurnal change of occurrence number of flow patterns. (a)autumn, (b)winter.*

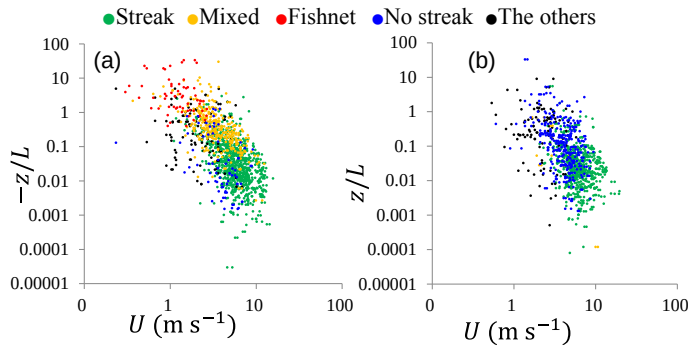


*Fig. 5 Stability and horizontal wind velocity of each flow pattern.(a)neutral and unstable, (b)stable.*

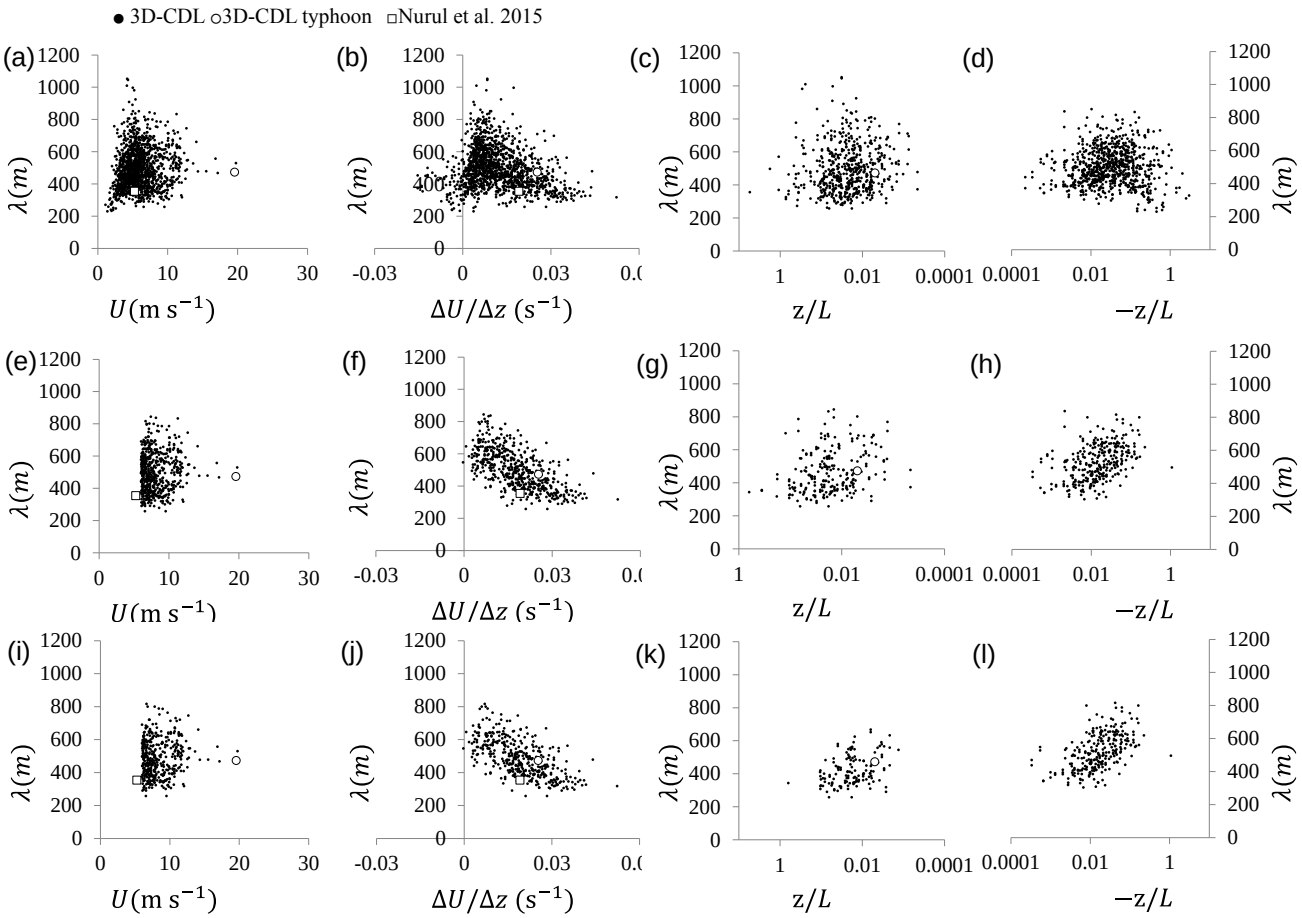


*Fig. 6 Spacing of streaky patterns and horizontal velocity, wind shear and stability.(a)(b)(c)(d)all cases, (e)(f)(g)(h)*cases when $U$ is larger than $6\,m\,s^{-1}$, (*i)(j)(k)(l)*cases when $U$ is larger than $6\,m\,s^{-1}$, excluding the cases around sunset time (16:00-20:00 in local time). Open circle *is observed during a typhoon which passed by the observation site on 30th Sep 2012*, Open square is *a numerical simulation, which resolved the urban buildings with 2m grid (Nurul 2015) using large eddy simulation model.*

**Acknowledgment**

This work was supported by JSPS KAKENHI Grant Numbers 25249066.

**References**

Adrian, R. J., Balachandar, S., and Lin, Z. C., 2001: Spanwise growth of vortex structure in wall turbulence. KSME international journal, 15, 1741-1749.

Castillo, M. C., Inagaki, A., and Kanda, M., 2011: The effects of inner-and outer-layer turbulence in a convective boundary layer on the near-neutral inertial sublayer over an urban-like surface. *Boundary-layer meteorology*, **140(3)**, 453-469.

Deardorff, J. W., 1972: Numerical Investigation of Neutral and Unstable Planetary Boundary Layers. *J. Atmos. Sci*., **29**, 91–115.

Khanna, S. and Brasseur, J. G., 1998: Three-dimensional buoyancy-and shear-induced local structure of the atmospheric boundary layer. *J. Atmos. Sci*., **55**, 710-743.

Moeng, C-H. and Sullivan, P. P., 1994: A comparison of shear-and buoyancy-driven planetary boundary layer flows. *J. Atmos. Sci*., **51**, 999-1022.

Sykes, R. I. and Henn, D. S., 1989: Large-Eddy Simulation of Turbulent Sheared Convection. *J. Atmos. Sci*., **46,** 1106–1118.

Newsom, R., Calhoun, R., Ligon, D., and Allwine, J., 2008: Linearly organized turbulence structures observed over a suburban area by dual-Doppler lidar. *Boundary-layer meteorology*, **127(1)**, 111-130.

Nurul, H. A., Inagaki, A., Kanda, M., Onodera,N., and Aoki, T., 2015: Spatial Distribution of the Gust Index over an Urban Area in Tokyo. *The 9th international conference on urban climate*, Toulouse, France.